Surface & Coatings Technology 422 (2021) 127559

Contents lists available at ScienceDirect

Surface & Coatings Technology

journal homepage: www.elsevier.com/locate/surfcoat

Estimation of coating thickness in electrostatic spray deposition by machine learning and response surface methodology

Uma Maheshwera Reddy Paturi [a,*], N.S. Reddy [b], Suryapavan Cheruku [a], Suresh Kumar Reddy Narala [c], Kwon Koo Cho [d], M.M. Reddy [e]

[a] Department of Mechanical Engineering, CVR College of Engineering, Hyderabad 501510, Telangana, India
[b] School of Materials Science and Engineering, Gyeongsang National University, Jinju 52828, South Korea
[c] Department of Mechanical Engineering, BITS-Pilani Hyderabad Campus, Hyderabad 500078, Telangana, India
[d] Department of Materials Engineering and Convergence Technology & RIGET, Gyeongsang National University, Jinju 52828, South Korea
[e] Department of Mechanical Engineering, Faculty of Engineering and Science, Curtin University Malaysia, Miri, Malaysia

ARTICLE INFO

Keywords:
Electrostatic spray deposition
Coating thickness
Artificial neural network
Support vector machine
Genetic algorithm
Response surface methodology

ABSTRACT

To improve the quality and productivity of the process or system before resorting to expensive and laborious experimental tests, it is essential to model and predict the system performance concerning its operational parameters. Predictive modeling and parameter optimization through machine learning techniques has been the most advantageous process and are the best alternative to the conventional statistical tools. In this work, carbide cutting tool inserts were coated with molybdenum disulfide (MoS_2) solid lubricant utilizing the electrostatic spray deposition (ESD) process. The optimum artificial neural network (ANN) model with 3-6-6-1 architecture includes 0.6 momentum term and 0.3 learning rate with attained mean squared error (MSE), absolute error in prediction (AEP) of trained and test data are 0.000334, 0.197, and 0.543, respectively. The support vector machine (SVM) hyperplane parameters are optimized using the Bayesian optimization technique, and after 90 evaluations, the model with the least error is used for predicting ESD coating thickness. The coating thickness predictions from ANN and SVM models were related to the response surface methodology (RSM) model predictions. From the results presented, the correlation coefficient (*R-value*) between experimental results and model predictions for ANN and SVM are 0.979 and 0.991, respectively, whereas, for RSM, it is 0.919. In addition, a genetic algorithm (GA) has been employed to establish the optimum conditions for the ESD deposition parameters. The presented SVM and GA method would support rapid and precise estimate and optimization of coating thickness in the ESD process.

1. Introduction

The ESD technique is complex due to operational parameters like applied electrical potential, air pressure, substrate distance, flow rate, and coating time [1]. The growing demands for ESD coating system performance in terms of achievable coating thickness, bonding strength, deposition efficiency, and cost have made it inevitably put a great deal of effort into controlling the critical parameters in the coating process [2]. For these reasons, few attempts using statistical techniques have been put into a mandate to optimize process performance and determine the significant parameter affecting the coating deposition technique [3]. Statistical design approaches are commonly applied to industrial powder coating processes to comprehend the effectiveness of process input parameters on coating efficacy and optimize the process conditions [4].

Some studies on utilizing statistical approaches such as Taguchi and orthogonal design methods, analysis of variance (ANOVA), and regression modeling for optimizing ESD coating process parameters were reported in the relevant literature. Paturi and Narala [5] applied the Taguchi design method and ANOVA to comprehend the complex ESD process parameters, interpret the experimental results, and show their influence on the surface quality of coatings. Nukala et al. [6] employed a conventional design of experiments (DOE) approach in electrostatic powder coating experiments to produce drug-coated stents. Barletta et al. [7] used the DOE statistical approach with ANOVA to understand the influence of ESD process factors on electrostatically charged epoxy-polyester powder paints. Though few mathematical and conventional

* Corresponding author.
E-mail address: maheshpaturi@gmail.com (U.M.R. Paturi).

https://doi.org/10.1016/j.surfcoat.2021.127559
Received 26 May 2021; Received in revised form 24 July 2021; Accepted 26 July 2021
Available online 28 July 2021

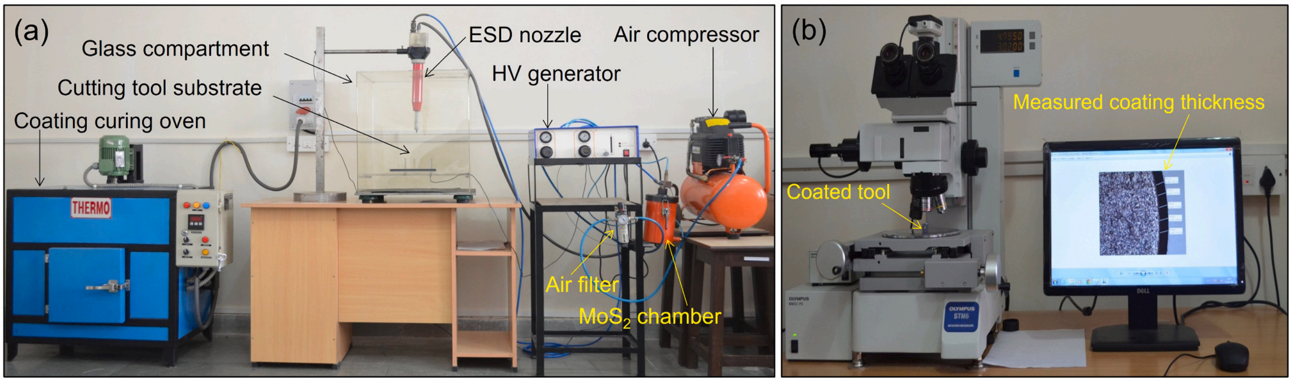

Fig. 1. (a) ESD coating experimental setup, and (b) coating thickness measurement.

statistical models are used in parameter optimization, applying these methods in ESD coating is not significantly beneficial, as noticeable from their limitation to the only lesser group of input conditions. Because of the nonlinear behavior among the coating process parameters, machine learning approaches as an alternative to the conventional statistical method have gained some attention in modeling and predicting the process input and output relation [8,9]. Besides, the machine learning approach is established to be exceptionally useful in process modeling of several other fields; such as manufacturing processes [10,11], automobile applications [12], material science [13], chemical process [14], tissue engineering [15], biological application [16], thermal engineering [17], bio-diesel production [18], medical science [19,20], aviation [21], nuclear engineering [22], food engineering [23], business [24], agricultural research [25], and power sector [26]. From the literature review, it can be concluded that machine learning techniques are the subject of interest in current time due to their excellent capabilities in modeling and prediction of process performance of complex nonlinear operations and engineering systems.

In addition to successful applications in above mentioned fields, the machine learning approach has been potentially applied in different areas of surface engineering [8]. S. Kamnis et al. [27] employed the ANN method to model coating microhardness with the power spectrum of airborne acoustic emissions as inputs in high velocity oxygen-fuel thermal coating deposition process. The work has concluded that the ANN enabled easy monitoring of coating deposition process based on airborne acoustic emissions and helped detect process flaws causing poor spraying conditions. Barletta et al. [28] modeled electrostatic fluid bed process using SVM for predicting the coating thickness. With an *R-value* of 0.996 for train data and 0.994 for test data, the author has predicted the coating thickness with high accuracy and suggested that machine learning can be the best choice for modeling the electrostatic fluid bed process. In another study by Shozib et al. [29], different machine learning methods such as ANN, SVM, Random Forest, and extra tress methods were employed to model and optimize electroless Ni-P-TiO_2 composite coating microhardness. The results presented show a high prediction capability of models with an *R-value* of 0.9447. Similarly, few other research works found in the literature have demonstrated the advantage of using machine learning methods in surface engineering applications [30–32].

However, to the best of our general knowledge, the literature review emphasized that utilizing the machine learning approaches in the ESD coating process remains scarce in the relevant literature. Hence, the primary motivation behind this study is to promote and develop the machine learning model (ANN and SVM) for the prediction of coating thickness in a nonlinear ESD process and relate the same with the results predicted by the conventional RSM model. Also, a GA-based machine learning approach has been implemented to optimize ESD process input parameters and obtain desired coating thickness. In modeling, real-time experimental data determined from the ESD process has been utilized. The effect of coating process parameters and their influence on coating thickness is discussed.

2. Experimental details

MoS_2 (molybdenum disulfide) solid lubricant supplied by Dow Corning Corp., the UK, with an average particle size of 0.7 μm, a density of 4.8 g/cc, and purity of about 98% was used as coating powder in preparation of ESD coatings on carbide cutting tool inserts. Phenolic resin powder particles with an average size of 2 μm and a density of 0.36 g/cc was used as a binding material in composition with the solid lubricant. The ESD coating experimental procedure presented in earlier work is adopted in the present study [33]. The ESD coating experimental setup with a sample measure of coating thickness on deposited cutting tool substrates using the tool maker's microscope (Olympus, STM6) is shown in Fig. 1. In this work, an orthogonal array with 27 rows, L27 (3^{13}) was used to plan the ESD experimental trials. Total experimental tests conducted using three levels for each selected control factor electric potential, powder feed pressure, and distance between nozzle tip to the substrate are illustrated in Table 1. To make the inevitable repeatability and least error, every test was performed three times. The mean coating thickness of three trials has been taken as the performance parameter.

3. Modeling

3.1. ANN modeling

The artificial neural network is a machine learning algorithm, parallel distributed processing model, and connectionist system. ANN utilizes a set of mathematical nodes (neurons) and interconnected links among nodes to transfer signals and frame the functional relationship in complex problems. Usually, a neural network model contains three layers, specifically, the input layer, one or more hidden layers, and the output layer. Each input neuron is input from actual data sets of the system or process and does not involve any information processing. The input neuron is linked with a connection that multiplies its strength by link weight to form the product. Then its output can be specified into other connected neurons by using a threshold function as represented in Eq. (1).

$$V_k = \sum_{j=0}^{n} x_j \, w_{kj} \tag{1}$$

where x_j stands for input and w_{kj} stands for connecting weight from neuron j to k.

For each tested data set, the strength of network or weight values is updated based on the backpropagation algorithm by comparing the error between the network output and target values. This procedure continues until the desired error (set minimum error) is achieved. The error between target output (t_p) and actual or fitted output (y_p) is

Table 1
Assignment of levels to the factors used in ESD experiments.

Control factors	Levels		
	1	2	3
Electric potential (kV)	50	70	90
Solid lubricant powder feed pressure (bar)	0.5	1.0	1.5
Distance between nozzle tip to the substrate (mm)	140	160	180

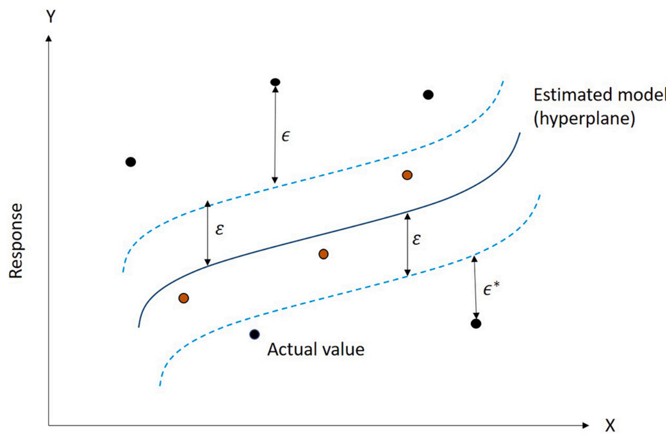

Fig. 2. A general view of SVM regression nonlinear model.

calculated according to Eq. (2). While updating network weight values, the learning rate and momentum term are selected based on the gradient descent function represented by Eq. (3).

$$E_p = \frac{1}{2}\sum \left(t_p - y_p\right)^2 \tag{2}$$

$$\Delta \mathrm{w_{ij}}\ (\mathrm{n}) = -\eta \sum\nolimits_{\mathrm{t}=0}^{\mathrm{n}} \alpha^{\mathrm{n-t}} \frac{\partial \mathrm{E(t)}}{\partial \mathrm{w_{ij}(t)}} \tag{3}$$

where η stands for learning rate, α stands for momentum term and $\frac{\partial E(t)}{\partial w_{ij}(t)}$ stands for the gradient.

ANN architecture comprises three layers (input, hidden, and output), learning rate, and momentum term. The input layer consists of three neurons with electric potential, feed pressure, substrate distance, and the output layer with only one neuron, namely, coating thickness. The ESD test data of this work has been split into training, test, and validation data groups in 6:3:1 share. The random division method was opted for dividing the given data. The ANN training comprises optimization of hidden layers, number of neurons in each hidden layer, learning rate, momentum term, and iterations. Several neural network models were generated with the current 27 experimental results. In ANN modeling, Levenberg Marquardt's training algorithm (*trainlm*) with hyperbolic tangent sigmoid transfer function *tansig* was employed in both hidden and output layers. As *logsig* and *ReLU* activation functions are restricted to the problems with range 0 to 1 and 0 to infinity respectively, the current work opted *tansig* as activation function concerning the input/output normalized values −1 to +1. Moreover, *tansig* activation function has been highly effective in establishing nonlinear relationships,

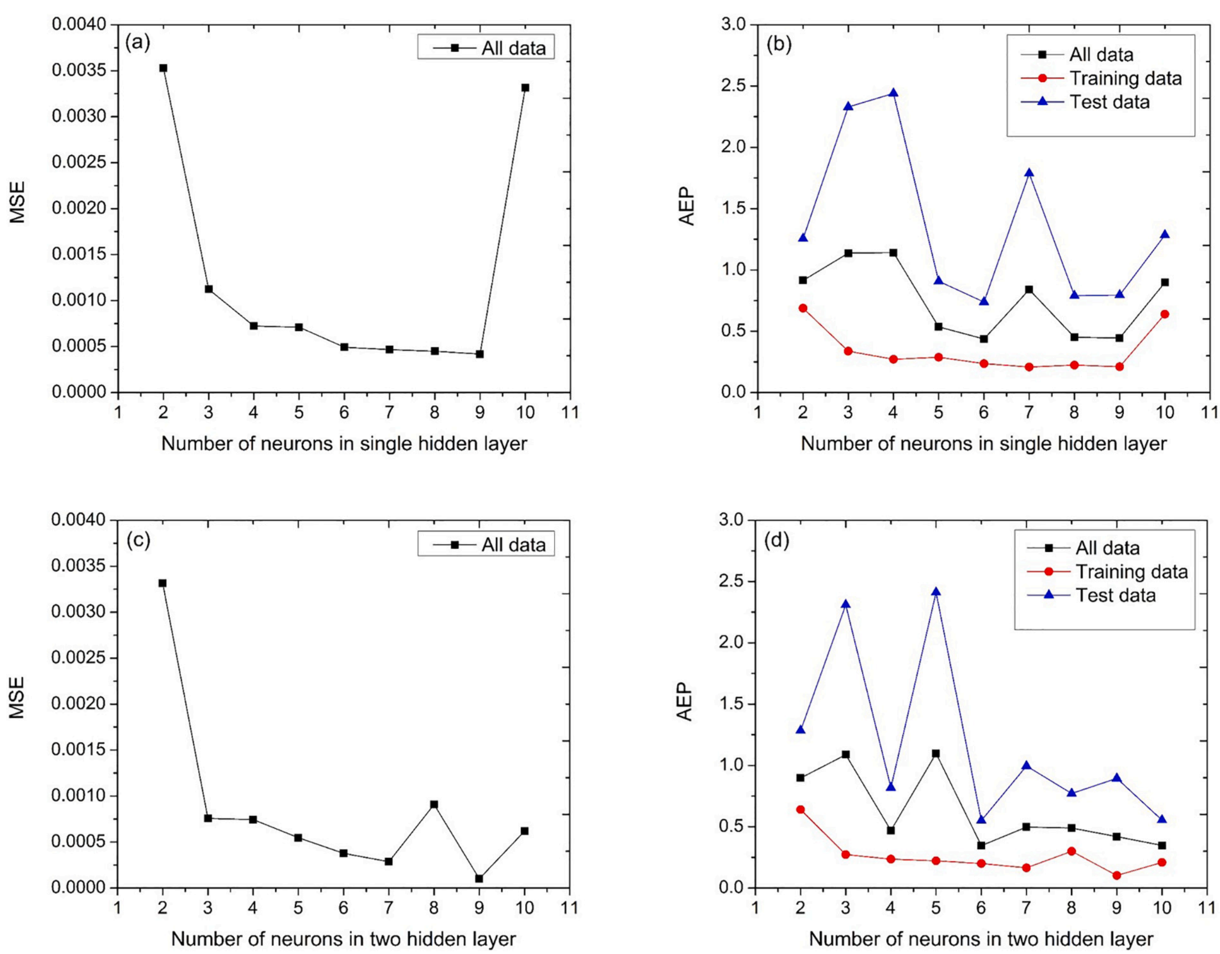

Fig. 3. MSE and AEP against varying neurons in the single and double hidden layer.

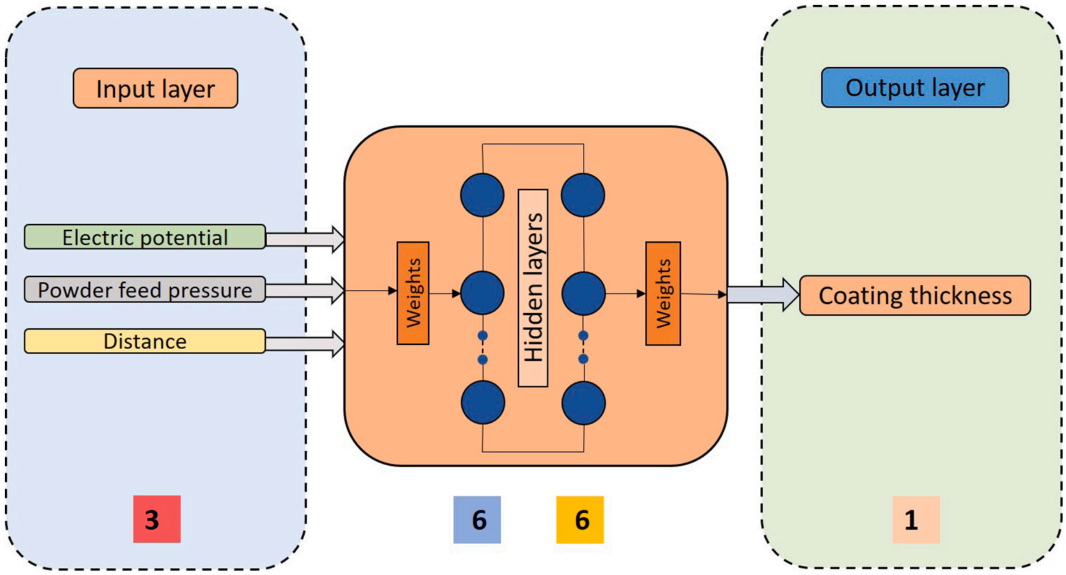

Fig. 4. Optimum neural network architecture with 3–6–6-1 topology.

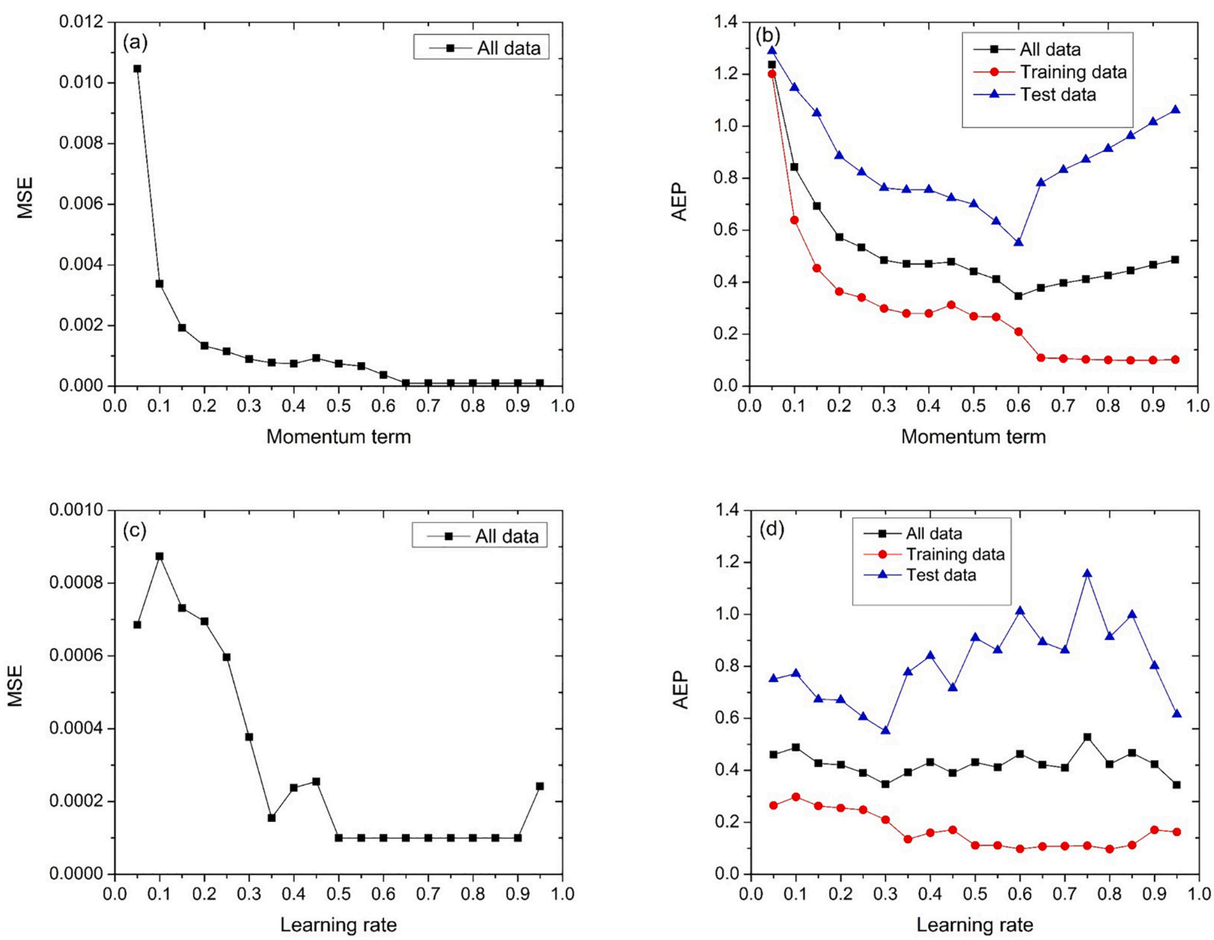

Fig. 5. MSE and AEP against varying momentum terms and learning rate.

especially when the data comprises negative values. The neural network model was trained with a feed-forward backpropagation learning algorithm. MATLAB, the mathematical computing software, has been employed in the training and testing of ANN architecture. The optimal ANN model was identified based on MSE and AEP results of test data.

The MSE and AEP calculations are carried out using Eqs. (4) and (5), respectively.

$$MSE = \frac{1}{N}\sum_{i=1}^{N}(t_i - td_i)^2 \tag{4}$$

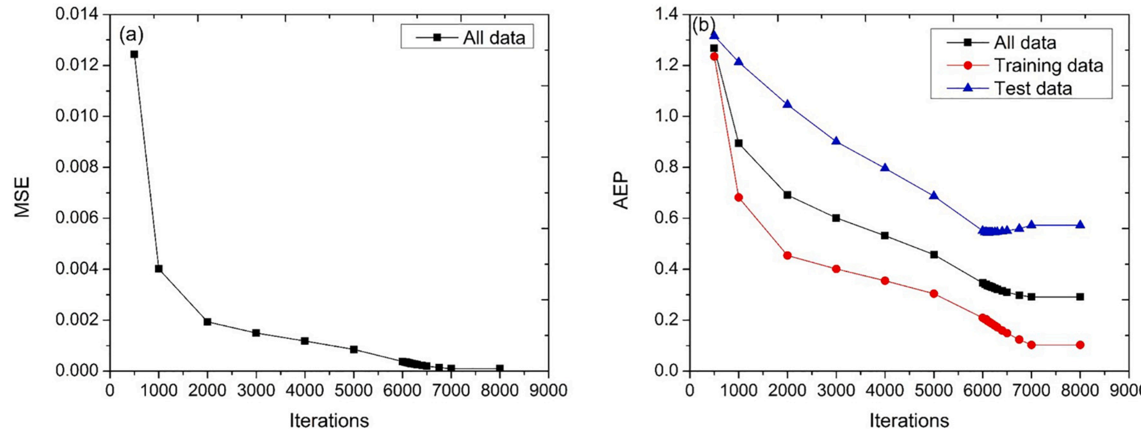

Fig. 6. MSE and AEP against the number of iterations with 3–6–6-1 architecture.

$$AEP = \frac{1}{N}\sum_{i=1}^{N}(|t_i - td_i|) \tag{5}$$

where, t_i denotes the targeted data, td_i denotes the model predicted data, and N denotes the size of available data.

To accelerate the training procedure and enhance the network performance, the input data sets as represented with electric potential, feed pressure, and substrate distance and output data set as represented with coating thickness were normalized between −1 and + 1. The ith normalized input/output dataset is estimated using Eq. (6).

$$D_{norm} = 2\times\frac{D_i - D_{min}}{D_{max} - D_{min}} - 1 \tag{6}$$

where D_{norm} denotes the ith normalized input/output dataset, D_i denotes the ith raw input/output dataset, while D_{min} and D_{max} are the minimum and maximum raw input/output datasets.

3.2. SVM modeling

SVM modeling has been carried out in MATLAB software by executing *fitrsvm* function. A generalized view of the SVM regression nonlinear model is presented in Fig. 2. As hyperplane parameters tuning is the most crucial step in SVM modeling, the Bayesian optimization technique is implemented for ESD process parameter optimization. Data division is carried out utilizing a 5-fold cross-validation approach, and the kernel function chosen is Gaussian. Initially, standardization of data was carried out to decrease the complexity, and modeling has been performed with the number of evaluations as 90. The developed model is then used to predict the coating thickness, and the model's performance is assessed with the aid of *R-value* between predicted thickness and experimental thickness value. Also, the model is validated by predicting the responses for three new different data sets obtained from the experimental results.

3.3. RSM modeling

Statistical based response surface method (RSM) is the most widely used tool in process modeling and optimization. The relationship among the response variable and independent parameters is explored. A systematic approach to model the correlation among the process output and its control factors in any engineering application would involve a great deal of work, which can be reduced to a reasonable extent using the RSM technique. RSM involves regression analysis, statistical and mathematical-based study, and experimental examinations. RSM utilizes a sequence of experiments to establish the optimal response of the system or determine the range of operational factors to extend the process improvement.

In the current paper, the quadratic regression relation established based on RSM predicts the ESD process coating thickness. The relationship generated between independent input variables (electric potential, powder feed pressure, and distance between nozzle tip to the substrate) with one desired dependent variable (coating thickness) is expressed with Eq. (7).

$$y = \beta_o + \beta_1 x_1 + \beta_2 x_2 + \beta_3 x_3 + \beta_{12} x_1 x_2 + \beta_{23} x_2 x_3 + \beta_{31} x_3 x_1 + \beta_{11} x_1^2 + \beta_{22} x_2^2 + \beta_{33} x_3^2 \tag{7}$$

where, y denotes the predicted result for each dependent variable, x_1, x_2, and x_3 are independent variables, β_o, β_1, β_2, and β_3 are model coefficients corresponding to the linear part of the model, β_{12}, β_{23} and β_{31} are the regression coefficients corresponding to cross part of the model, and β_{11}, β_{22} and β_{33} are coefficients corresponding to the quadratic part of the regression model.

3.4. Optimization using GA

Selecting the best input conditions for the ESD process plays a pivotal step in obtaining desired value of coating thickness. GA has been implemented in the current work to optimize the input parameters and get the required coating thickness. The MATLAB toolbox is used for GA optimization. The derived mathematical equation through RSM modeling is used as a fitness function with three variables: electric potential, solid lubricant power feed pressure, and distance between nozzle tip to the substrate, with the output being coating thickness. Based on the experimental data, lower and upper bounds have been opted. Optimum conditions for population size, population type, selection function, and the number of generations are chosen accordingly. Optimization is terminated when the average variation in the fitness value is lower than the given tolerance. The optimized input parameters and coating thickness value at those conditions are obtained and compared with the experimental results for validating the model performance.

4. Results and discussion

4.1. ANN modeling

Numerous factors need to be chosen when designing neural network architecture to match the given application. Among these factors are the input layer, output layer, network weight and nature of transfer function, etc. Hidden layer, neurons in each hidden layer, momentum term,

Table 2
Optimized SVM hyperplane parameters.

Hyperplane parameter	Value
Kernel function	Gaussian
Box constraint	211.76
Kernel scale	3.1504
Epsilon	0.0055965

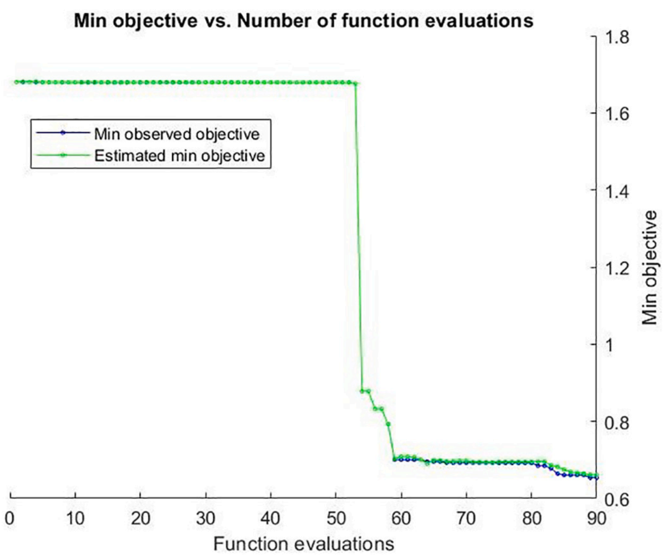

Fig. 7. Variation of objective value at the different number of evaluations.

learning rate, and the number of training iterations of the ANN model influence the performance. Hence, in the current study, 32 different architectures were studied by varying the above parameters to identify the optimum architecture. Fig. 3 shows MSE and AEP against different neurons in single and double hidden layers. It was noticed that the ANN model is more stable and converged with two hidden layers consisting of six neurons in every single hidden layer and displays a least average error of 0.551 among all other neurons considered in the study. Further, from the MSE and AEP performance indicators of the trained data, network structure 3-6-6-1 with 0.6 as momentum term and 0.3 as learning rate is the most confident and optimum ANN model. The optimal ANN architecture attained in this study is shown in Fig. 4.

The influence of momentum term and learning rate of optimum ANN model on the performance functions of MSE and AEP is presented in Fig. 5. The analysis was made on nine sets of momentum terms and learning rates ranging from 0.1 to 0.9. Fig. 5 shows the MSE and AEP of network predicted and targeted values for the training, testing, and all data considered versus varying momentum terms and learning rate. Based on the analysis, it is witnessed that low momentum term and high learning rate combinations do not offer satisfactory results for the trained and test data sets and the ANN architecture used. The minimum average absolute error in prediction can be seen with the momentum and learning rates of 0.6 and 0.3.

To comprehend how well the ANN architecture is optimal and avoid over-training, the model performance was again tested under several training iterations. MSE and AEP variation under different training iterations with optimal 3-6-6-1 ANN architecture corresponding to 0.6 momentum term and 0.3 learning rate is presented in Fig. 6. From Fig. 6, it was observed that after 6100 iterations, AEP for the test data started ultimately rising. In contrast, the average error of training data continuously falling and then reaches a stabilization value. Therefore, the network training was stopped at 6100 iterations, and the corresponding MSE and AEP for the training and test data are seen to be 0.000334, 0.197, and 0.54365, respectively.

4.2. SVM modeling

Optimization of hyperplane parameters is successfully carried out using the Bayesian optimization technique. Initially, 27 data set values have been standardized and divided according to the 5-fold cross-validation technique. After modeling the data with kernel function as Gaussian and maximum objective evaluations as 90, it has been found that the model with hyperplane parameter values as $C = 211.76$, kernel scale $= 3.1504$, and epsilon $= 0.005597$ resulted in the least error between estimated and observed objective value (Table 2). Fig. 7 depicts the variation of objective value during 90 evaluations. From Fig. 7, it can be observed that estimated and observed functional values are coinciding at the maximum number of instances, and the objective function value has kept decreasing with the increase in the number of evaluations. Thus, the best hyperplane parameters are determined using the Bayesian optimization technique.

The developed model is then used for predicting the ESD process coating thickness for 27 data sets. Relation between SVM predicted results and experimental results is judged using *R*-value. The results show that the model has generated a perfect fit for the given nonlinear data with an *R*-value of 0.990734, indicating significant harmony between experimental results and predicted values. Also, validation of the model is performed on three new datasets from the experimental results. The *R*-value has been observed to be 0.991 for all 30 dataset values, including validation data between experimental results and predicted response. Thus, a larger *R*-value of validation data validated the model's accurate performance. It can be concluded here that the established SVM model has shown excellent prediction capability in modeling coating thickness.

4.3. RSM modeling

In the present study, a statistical RSM model is developed. The calculated RSM relationship between the dependent response (coating thickness) and independent parameters (electric potential, feed pressure, and substrate distance) is presented by Eq. (8).

$$\begin{aligned}\text{Coating thickness} = & -48.7228 + 0.9488A + 6.7325B + 0.3156C \\ & -0.0059A^2 - 6.2978B^2 - 0.0008C^2 + 0.0393A*B \\ & -0.0007A*C + 0.0260B*C \end{aligned} \tag{8}$$

where *A* is electric potential, *B* is powder feed pressure, and *C* is the distance between nozzle tip to the substrate.

ANOVA and F-tests were conducted to identify the RSM model that best fits the whole data from which the data were tested and interpret input value and test values in a structured manner after a series of experimental runs. The ANOVA and F-test results for regression analysis are presented in Table 3.

From the *F*-test results, the *p*-value demonstrates that the regression equation, linear part, and square part are significant at an α-level of 0.05 (95% level of confidence). However, the interaction part seems to have not of substantial effect on the coating thickness. This is true because the estimated *p*-value is lower than the current significant level for the regression model; hence it agrees that the developed regression model fits the data quite well. In addition to this, the Anderson–Darling statistical test was also conducted to compare how well the known data is within normal probability distribution. The normal probability distribution of the residuals against the predicted coating thickness is shown in Fig. 8. The correlation between the predicted results and actual results displayed in Fig. 8 forms a nearly straight line. From the probability plot, it is observed that the sampling distribution is normal as the *p*-value for the Anderson–Darling statistical test is more than 'α' of 0.05 at reference confidence of level 95%. Thus, it suggests that the null hypothesis cannot be overlooked, indicating the RSM model designed for predictions of coating thickness in the ESD process is adequate.

Table 3
ANOVA results for the regression model.

Source	DF	SS	MS	F_{test}	*p*-Value
Regression	9	88.5673	9.8408	11.01	0.000*
Linear	3	35.786	8.9442	10.01	0.000*
Square	3	49.247	16.4157	18.36	0.000*
Interaction	3	3.535	1.1782	1.32	0.301*
Residual error	17	15.197	0.8939	–	–
Total	26	103.764	–	–	–

DF = degree of freedom, SS = sum of squares, MS = mean square.
* Significant.

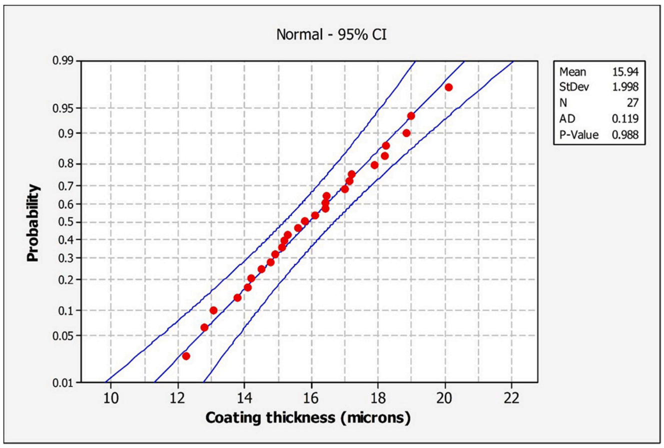

Fig. 8. Normal probability plot for coating thickness.

4.4. Optimum results

The coating deposition process parameters, powder feed pressure, electric potential, and nozzle tip to the substrate distance play a vital role in achieving the desired coating thickness and transfer efficiency. Hence, to investigate the optimal deposition process parameters and comprehend their significance on the overall thickness of the coatings, GA optimization is employed. The mathematical equation derived through RSM modeling has been opted as a fitness function for GA optimization. The conditions opted for GA implementation are shown in Table 4. Lower bounds are taken as level 1 factors of experimental data, and upper bounds are taken as level 3 factors of experimental data. Process optimization is carried out till the average deviation in the fitness value is under the given tolerance. Optimization is terminated at the 51st iteration, and the final fitness objective value obtained for coating thickness is 12.35. The optimal deposition process parameters for coating thickness are as follows: electric potential = 50 kV, powder feed pressure = 1.5 bar, and the distance between nozzle tip to the substrate = 140 mm. Variation of fitness value against the number of generations is presented in Fig. 9(a). Approximately at the 50th generation, the best fitness value, i.e., coating thickness is obtained. Fig. 9(b) depicts the best input parameter values that resulted in desired coating thickness. The best fitness value was observed at level 1 factor of electric potential and the nozzle tip to the substrate distance and level 2 factor of powder feed pressure. Hence, GA has been highly influential in optimizing the input parameters and yielding the required response value. Moreover, validation of GA results is performed by comparing them with experimental values. It is found that the error between GA fitness value and experimental value is only 3.44%, demonstrating the technique's excellent capability in nonlinear process optimization.

4.5. Effect of ESD process parameters

The influence of ESD process deposition process parameters on the coating thickness is presented. Fig. 10 shows 3D plots of the electrostatic coating experimental response versus all the operational variables. From the analysis of variance, it was observed that the percent contribution of each parameter on the overall thickness of coatings is as follows: electric potential factors (50.33%), powder feed pressure factors (17.73%), and distance between the nozzle tip to substrate factors (13.81%). The electric potential has the highest main effect on the coating thickness among all the deposition process parameters tested. Also, it observed that the electrical potential of other parameters greatly influenced the trend in coating thickness. An increase in coating thickness values was seen when the voltage changes from 50 to 70 kV. When electric potential changes from 70 to 90 kV, a moderate reduction in coating thickness was observed. This could be due to the surge in electrostatic forces, which in turn greatly affect the lubricant powder particles flow. Moreover, when the electric potential increases, the development of an electric field around the particles would be projected to rise. This shows that when electric potential is high, more charged particles transfer through the electric field and push near the tool substrate. As the number of charged particles push from the nozzle tip to substrate increases, the transfer efficiency of electrostatic spray deposition would be expected to increase. In addition to the above, change in powder feeding pressure also influences the thickness of coatings. In contrast, the difference in the distance between the nozzle tip to the substrate caused a slight variation in the coating thickness. This could be mostly due to the electrical field force determined from the electric potential set. The effect of gravitational force on particle movement is neglected because electrostatic forces on particle are more than the gravitational effects.

4.6. Confirmation tests

To verify the adequacy of the developed ANN, SVM, and RSM models, three confirmation trial experiments (Exp. No. 28 to 30 of Table 5), consisting of a combination of input process parameters that do not belong to the original plan of the experimental domain were performed. The ESD process conditions such as electric potential, powder feed pressure, and distance from the nozzle to substrate used in confirmation tests and comparison of measured and predicted results of coating thickness are illustrated in Table 5. The predicted coating thickness value from the developed and actual experimental values was compared, and the percentage error is calculated. From the confirmation results presented in Table 5, it was observed that the maximum calculated absolute error percentage between the SVM model and experimental results is 0.78%. In comparison, the same error with ANN and RSM models is 4.54% and 5.86%, respectively. Thus, the confirmation results demonstrate that the developed models correlate the relationship of the coating thickness between predictions and experimental results effectively and can be used to predict coating thickness.

4.7. Comparison of ANN, SVM, and RSM model predictions

ANN, SVM, and RSM model efficacies are assessed by comparing the model estimates with experimentally measured coating thickness results. The experimental and model prediction results for all 27 experiments and 3 unseen validation data sets and prediction errors are presented in Table 5. The developed model prediction capability was measured in terms of *R-value* and the average absolute error between experiential and model predicted thickness values. '*R*' is the most widely used statistical performance indicator to measure the significance of the regression model, i.e., the strength and degree of linear dependency between model-predicted and experimentally measured values. The *R-value* used in this paper is expressed by Eq. (9).

Table 4
GA optimization conditions.

Parameters	Conditions
Population size	50
Population type	Double vector
Number of generations	500
Selection function	Stochastic uniform
Lower bounds	[50 0.5 140]
Upper bounds	[90 1.5 180]

$$R = 1 - \frac{\sum_{i=1}^{N}\left(t_{m,i} - y_{p,i}\right)^2}{\sum_{i=1}^{N}\left(t_{m,i}\right)^2} \tag{9}$$

where $t_{m,i}$ denotes the experimentally measured value, $y_{p,i}$ denotes the model predicted value, and N denotes the size of data groups.

It is noticed from the results that developed models demonstrate a reasonable degree of linear dependency of fit among experimentally obtained results and model prediction results. Based on the R-values of different data sets (Fig. 11), the SVM model can provide a precise and accurate estimate of the coating thickness. From Fig. 11, an R-value of 0.97908 for all data is given by ANN whereas, for unseen validation data, it has shown 0.92103. The SVM model provides an R-value of 0.9907 for all data and 0.9912 for data with validation. On the other hand, the corresponding R-values with the RSM model are about 0.91953 and 0.88278, respectively. Thus, the larger values of R demonstrate that the association of the SVM model predictions to the experimentally obtained results is confirmed to be very high, and the SVM model is more approximate and fits the data well. Thus, the SVM approach is reasonably efficient in modeling and predicting the coating thickness in the ESD process.

Usually, the larger the correlation coefficient, the stronger the linear fit between two variables. A correlation coefficient value of zero means that there is no linear association between predicted and experimental results. A perfect linear relationship gives a correlation coefficient value of one. Sometimes a high R-value does not indeed indicate that the regression model performance is high since the over and under prediction tendency (bias) at different points can occur along the fitted regression line. Hence, in the present study, an unbiased statistical mean absolute error (Δ) is calculated by considering every data point error between the model and the experimentally measured value for judging the model effectiveness convincingly. For this, the mean absolute error percentage is estimated with the help of Eq. (10).

$$\Delta = \frac{1}{N}\sum_{i=1}^{N}\left|\frac{\left(t_{m,i} - y_{p,i}\right)}{t_{m,i}}\right| \times 100 \tag{10}$$

As it can be realized from Table 5, RSM, SVM, and ANN model predictions are demonstrated to be in reasonably convincing agreement when matched to the experimentally measured values except for some slight deviations. Further, it can be observed from Table 5 that SVM model predictions lead to the least absolute percentage error as compared to ANN and RSM model predictions. The maximum prediction errors for SVM, ANN, and RSM model with 27 data sets are about 7.3411%, 8.6%, and 12.37%, respectively. Moreover, the mean absolute

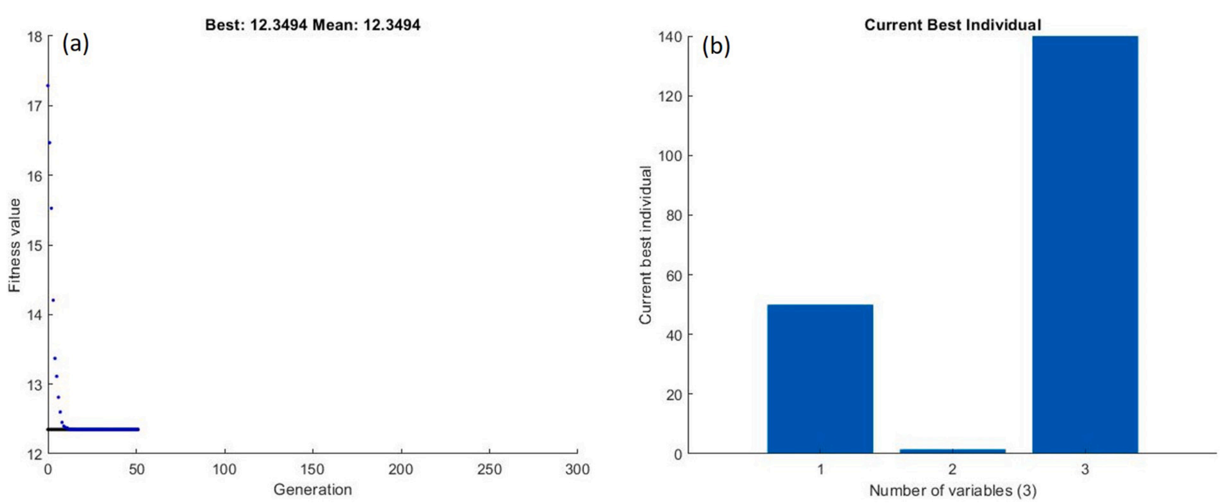

Fig. 9. (a) Variation of fitness value against the number of generations, and (b) Optimized input values.

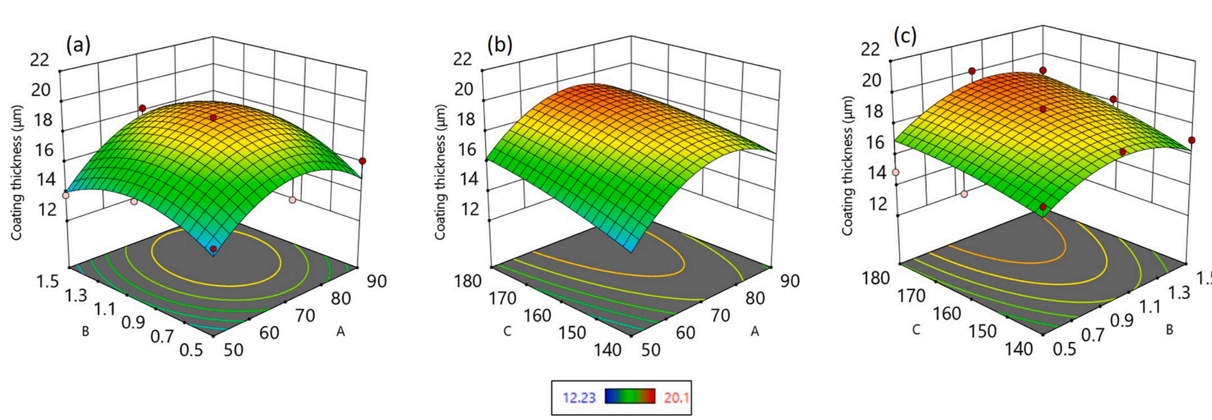

Fig. 10. Effect of process parameters (A: electric potential, B: powder feed pressure, and C: Distance between nozzle tip to the substrate) on coating thickness.

Table 5
ANN, SVM, and RSM model prediction comparisons with experimental measurements.

Exp. no.	Control factors			Experimentally measured coating thickness (μm)	Model predictions			Absolute error (%)		
	Electric potential (kV)	Powder feed pressure (bar)	Distance between nozzle tip to the substrate (mm)		ANN model	SVM model	RSM model	ANN model	SVM model	RSM model
1	50	0.5	140	12.23	12.45	12.23	12.17	1.79	0.045	0.49
2	50	0.5	160	14.2	13.96	14.19	13.24	1.69	0.038	6.76
3	50	0.5	180	15.6	15.62	15.59	13.67	0.12	0.031	12.37
4	50	1.0	140	13.07	13.20	13.07	13.61	0.99	0.034	4.13
5	50	1.0	160	15.2	14.74	15.19	14.94	3.02	0.032	1.71
6	50	1.0	180	16.45	16.51	16.45	15.63	0.36	0.032	4.98
7	50	1.5	140	12.79	13.28	12.78	11.91	3.83	0.032	6.88
8	50	1.5	160	13.77	13.69	13.76	13.50	0.58	0.048	1.96
9	50	1.5	180	14.08	14.05	14.07	14.45	0.21	0.023	2.62
10	70	0.5	140	16.4	16.03	16.08	15.41	2.25	1.914	6.03
11	70	0.5	160	15.3	15.62	15.62	16.21	2.09	2.113	5.94
12	70	0.5	180	14.9	15.53	14.90	16.36	4.22	0.048	9.79
13	70	1.0	140	17.9	18.01	17.90	17.25	0.61	0.031	3.63
14	70	1.0	160	19.0	19.44	18.99	18.31	2.31	0.045	3.63
15	70	1.0	180	20.1	19.76	19.43	18.72	1.69	3.307	6.86
16	70	1.5	140	17.0	16.33	16.99	15.94	3.94	0.041	6.23
17	70	1.5	160	18.21	18.10	18.21	17.25	0.6	0.030	5.27
18	70	1.5	180	18.86	19.06	18.65	17.93	1.06	1.097	4.93
19	90	0.5	140	14.5	15.02	14.50	13.94	3.58	0.037	3.86
20	90	0.5	160	16.12	15.83	14.93	14.46	1.79	7.341	10.29
21	90	0.5	180	14.76	16.03	14.76	14.33	8.6	0.036	2.91
22	90	1.0	140	15.8	15.63	15.79	16.17	1.07	0.046	2.34
23	90	1.0	160	17.12	17.03	17.20	16.95	0.52	0.468	0.99
24	90	1.0	180	18.24	18.32	18.23	17.08	0.43	0.022	6.35
25	90	1.5	140	15.1	15.22	15.10	15.26	0.79	0.040	1.05
26	90	1.5	160	16.4	16.27	16.39	16.29	0.79	0.038	0.67
27	90	1.5	180	17.2	17.35	17.20	16.68	0.87	0.031	3.02
28	**50**	**1.5**	**150**	**13.32**	**13.69**	**13.32**	**12.78**	**2.77**	**0.049**	**4.05**
29	**60**	**1.5**	**180**	**15.85**	**16.57**	**15.95**	**16.78**	**4.54**	**0.644**	**5.86**
30	**80**	**1.25**	**170**	**18.14**	**18.79**	**18.28**	**18.46**	**3.58**	**0.782**	**1.76**

Note: Data sets of Exp. No. 1–18, 19–27, and 28–30 are used in training, testing, and confirmation respectively.

error between the SVM model and experimentally obtained results is 0.61%, while the same value calculated for ANN and RSM models are 1.84% and 4.65%, respectively (Table 6). The statistical *R-value* and mean absolute error values attained by SVM, ANN, and RSM model are reasonably acceptable for coating thickness prediction in the ESD process. Further, machine learning techniques (ANN and SVM) are more precise in coating thickness prediction when compared to the statistical RSM model. Thus, ANN and SVM models are expected to be beneficial in curtailing time-consuming and expensive practical tests of the ESD coating process.

In summary, as noticed clearly from *R*-value and mean absolute error results comparison, SVM model prediction capability is superior to ANN and RSM models. This is a fact since *R*-value acquired with the SVM model is as close as 1 (0.991). It can be concluded here that the output demonstrates that the SVM model relates the input elements with response parameter quite efficiently and consequently give an accurate estimate of linear dependence of fit between model and experimental results. Thus, the established SVM model is more precise and reliable in the prediction of coating thickness when matched to the ANN and RSM models for the given input to output configuration. Moreover, there is also a greater scope for implementing reverse configuration (output to input) using partial dependence plots where the optimum values of input parameters can be predicted with the given output [34].

5. Conclusion

In the present paper, an experimental and computational approach for the ESD coating process has been presented. The coating thickness values for different levels of electric potential, powder feed pressure, and distance between nozzle tip to the substrate were measured from real-time ESD experiments. Later, ANN, SVM and RSM techniques were used for ESD process modeling, and the GA approach is used for optimizing coating thickness. Finally, the prediction efficiency of developed machine learning models (ANN and SVM) was compared with the statistical RSM model. The key conclusions of the work are listed below:

- Based on the MSE and AEP of the trained data, the optimum ANN model was achieved with a 3-6-6-1 architecture with 0.6 momentum term, 0.3 learning rate, and 6100 iterations.
- Bayesian optimization enabled quick and accurate determination of optimal hyperplane parameters in SVM modeling.
- The effect of different input parameters on coating thickness has been determined from the ANOVA results. It is found that Electric potential is the most influencing parameter with a percentage contribution of 50.33%, followed by power feed pressure and distance between nozzle tip to the substrate.
- GA is highly beneficial in optimizing the input parameters of the ESD coating deposition process and provided the desired coating thickness with a very low prediction error of 3.44%.
- Among all the models, the SVM prediction coating thickness values are confirmed to be in persuasive agreement when matched to the experimentally measured values with an *R*-value of 0.991 and mean absolute error of 0.61%.
- Thus, the results of this study demonstrate that the use of SVM modeling and GA optimization approach can endow a precise estimate of coating thickness as well as curtailing time-consuming and expensive ESD experimental investigations.

CRediT authorship contribution statement

Uma Maheshwera Reddy Paturi: Conceptualization, Methodology, Validation, Formal analysis, Investigation, Writing – original draft. **N.S. Reddy:** Data curation, Writing – review & editing. **Suryapavan Cheruku:** Software. **Suresh Kumar Reddy Narala:** Resources. **Kwon Koo Cho:** Visualization. **M. Mohan Reddy:** Supervision.

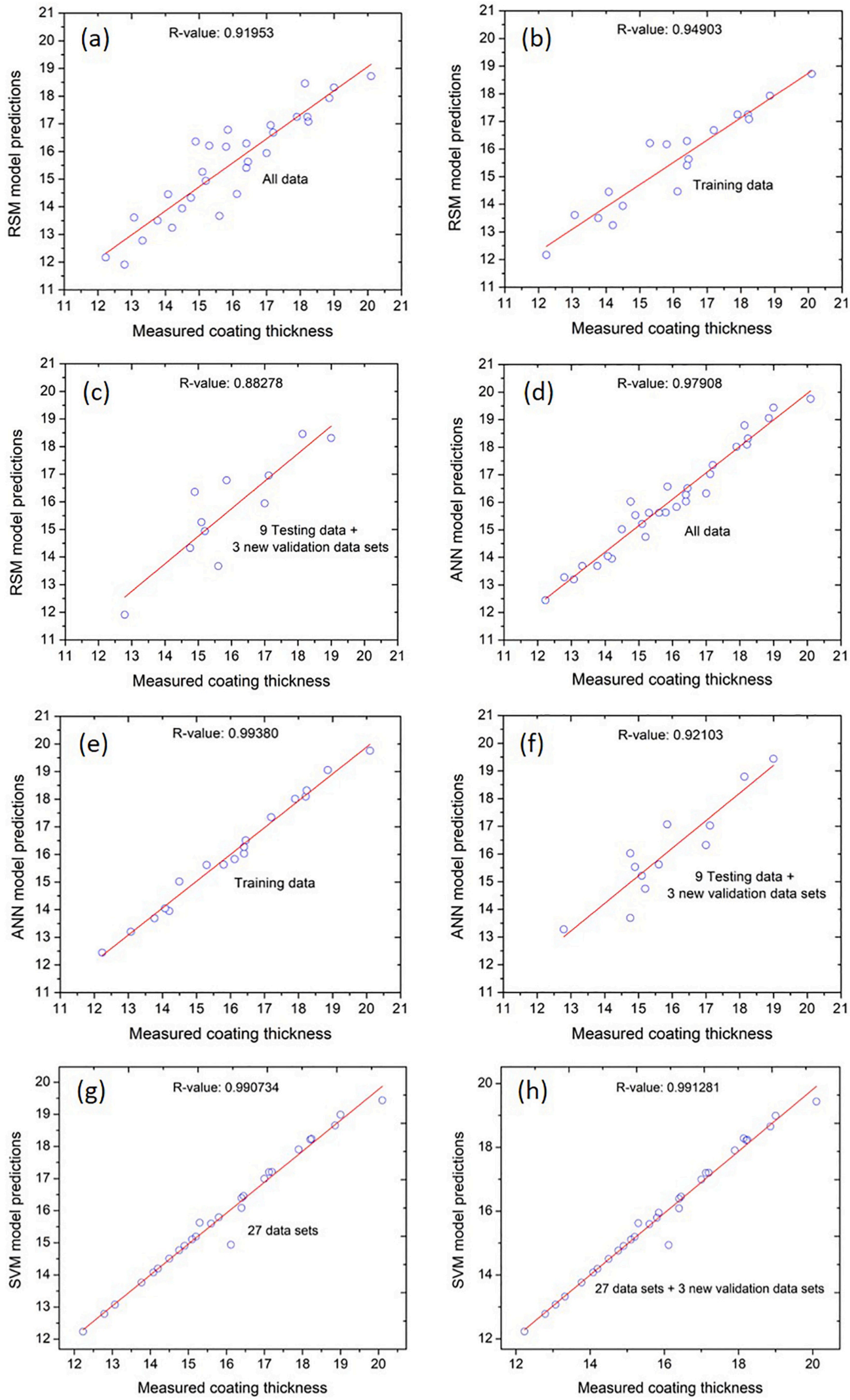

Fig. 11. Comparison of ANN, SVM, and RSM models performance for different seen and unseen data sets.

Table 6
Summary of the performance of techniques.

S. no.	Technique	*R*-value	(Δ)
1	SVM	0.991	0.61%
2	ANN	0.979	1.84%
3	RSM	0.919	4.65%

Declaration of competing interest

The authors declare that they have no known competing financial interests or personal relationships that could have appeared to influence the work reported in this paper.

Acknowledgement

Authors would like to extend their thanks to all the support needed for this study. Also, N.S. Reddy acknowledges YSJ and SCAN for the inspiration.

References

[1] M. Barletta, A. Gisario, S. Guarino, Modelling of electrostatic fluidized bed (EFB) coating process using artificial neural networks, Eng. Appl. Artif. Intell. 20 (2007) 721–733, https://doi.org/10.1016/j.engappai.2006.06.013.
[2] C. Ghanshyam, S. Bagchi, P. Kapur, Optimization of spray parameters in the fabrication of SnO_2 layer using electrostatic assisted deposition technique, J. Electrost. 71 (2013) 68–76, https://doi.org/10.1016/j.elstat.2012.10.001.
[3] V. Goud, A. Ramasamy, A. Das, D. Kalyanasundaram, Box-Behnken technique based multi-parametric optimization of electrostatic spray coating in the manufacturing of thermoplastic composites, Mater. Manuf. Process. 34 (2019) 1638–1645, https://doi.org/10.1080/10426914.2019.1666991.
[4] N. Arunkumar, P. Venkatesh, K.S. Srinivas, S. Kaushik, Response surface modeling and optimization of single axis automatic application of automotive polyurethane coatings on plastic components, Int. J. Adv. Manuf. Technol. 63 (2012) 1065–1072, https://doi.org/10.1007/s00170-012-3970-1.
[5] U.M.R. Paturi, S.K.R. Narala, Electrostatic solid lubricant coatings: optimization of process parameters and performance in tribological tests, Solid State Phenom. 266 (2017) 64–68, https://doi.org/10.4028/www.scientific.net/SSP.266.64.
[6] R.K. Nukala, H. Boyapally, I.J. Slipper, A.P. Mendham, D. Douroumis, The application of electrostatic dry powder deposition technology to coat drug-eluting stents, Pharm. Res. 27 (1) (2010) 72–81, https://doi.org/10.1007/s11095-009-0008-y.
[7] M. Barletta, A. Gisario, V. Tagliaferri, Electrostatic spray deposition (ESD) of polymeric powders on thermoplastic (PA66) substrate, Surf. Coat. Technol. 201 (2006) 296–308, https://doi.org/10.1016/j.surfcoat.2005.11.120.
[8] U.M.R. Paturi, S. Cheruku, S.R. Geereddy, Process modeling and parameter optimization of surface coatings using artificial neural networks (ANNs): state-of-the-art review, Mater. Today Proc. (2020), https://doi.org/10.1016/j.matpr.2020.08.695.
[9] O. Altay, T. Gurgenc, M. Ulas, C. Özel, Prediction of wear loss quantities of ferro-alloy coating using different machine learning algorithms, Friction. 8 (2020) 107–114, https://doi.org/10.1007/s40544-018-0249-z.
[10] H. Elhoone, T. Zhang, M. Anwar, S. Desai, Cyber-based design for additive manufacturing using artificial neural networks for industry 4.0, Int. J. Prod. Res. 58 (2020) 2841–2861, https://doi.org/10.1080/00207543.2019.1671627.
[11] U.M.R. Paturi, S. Cheruku, Application and performance of machine learning techniques in manufacturing sector from the past two decades: a review, Mater. Today Proc. (2020), https://doi.org/10.1016/j.matpr.2020.07.209.
[12] A. Shebani, S. Iwnicki, Prediction of wheel and rail wear under different contact conditions using artificial neural networks, Wear. 406-407 (2018) 173–184, https://doi.org/10.1016/j.wear.2018.01.007.
[13] S. Feng, H. Zhou, H. Dong, Using deep neural network with small dataset to predict material defects, Mater. Des. 162 (2019) 300–310, https://doi.org/10.1016/j.matdes.2018.11.060.
[14] Z. Zhang, J. Zhao, A deep belief network based fault diagnosis model for complex chemical processes, Comput. Chem. Eng. 107 (2017) 395–407, https://doi.org/10.1016/j.compchemeng.2017.02.041.
[15] B.S. Reddy, K.H. In, B.B. Panigrahi, U.M.R. Paturi, K.K. Cho, N.S. Reddy, Modeling tensile strength and suture retention of polycaprolactone electrospun nanofibrous scaffolds by artificial neural networks, Mater. Today Commun. 26 (2021), 102115, https://doi.org/10.1016/j.mtcomm.2021.102115.
[16] M. Sadeghassadi, C.J.B. Macnab, B. Gopaluni, D. Westwick, Application of neural networks for optimal-setpoint design and MPC control in biological wastewater treatment, Comput. Chem. Eng. 115 (2018) 150–160, https://doi.org/10.1016/j.compchemeng.2018.04.007.
[17] S. Chowdhury, S. Anand, Artificial neural network based geometric compensation for thermal deformation in additive manufacturing processes, ASME 2016 11th Int. Manuf. Sci. Eng. Conf. MSEC 2016. 3 (2016) 1–10. doi:https://doi.org/10.1115/MSEC20168784.
[18] E. Betiku, O.R. Omilakin, S.O. Ajala, A.A. Okeleye, A.E. Taiwo, B.O. Solomon, Mathematical modeling and process parameters optimization studies by artificial neural network and response surface methodology: a case of non-edible neem (Azadirachta indica) seed oil biodiesel synthesis, Energy. 72 (2014) 266–273, https://doi.org/10.1016/j.energy.2014.05.033.
[19] O.W. Samuel, G.M. Asogbon, A. Sangaiah, P. Fang, G. Li, An integrated decision support system based on ANN and Fuzzy_AHP for heart failure risk prediction, Expert Syst. Appl. 68 (2017) 163–172, https://doi.org/10.1016/j.eswa.2016.10.020.
[20] S.M. Anwar, M. Majid, A. Qayyum, M. Awais, M. Alnowami, M.K. Khan, Medical image analysis using convolutional neural networks: a review, J. Med. Syst. 42 (2018) 1–13, https://doi.org/10.1007/s10916-018-1088-1.
[21] TV Sanli, G. Ercan, D. Coker, A. Kayran, Development of artificial neural network based design tool for aircraft engine bolted flange connection subject to combined axial and moment load. IMECE2017-70448, (2018) 1–11. doi:https://doi.org/10.1115/IMECE2017-70448.
[22] M.R. Lee, J.H. Lee, J.T. Kim, Condition monitoring of a nuclear power plant check valve based on acoustic emission and a neural network, J. Press. Vessel Technol. Trans. ASME. 127 (2005) 230–236, https://doi.org/10.1115/1.1991880.
[23] N. Vásquez, C. Magán, J. Oblitas, T. Chuquizuta, H. Avila-George, W. Castro, Comparison between artificial neural network and partial least squares regression models for hardness modeling during the ripening process of Swiss-type cheese using spectral profiles, J. Food Eng. 219 (2018) 8–15, https://doi.org/10.1016/j.jfoodeng.2017.09.008.
[24] J.R. Coakley, C.E. Brown, Artificial neural networks in accounting and finance: modeling issues, Int. J. Intell. Syst. Accounting, Financ. Manag. 9 (2000) 119–144, https://doi.org/10.1002/1099-1174(200006)9:2<119::aid-isaf182>3.0.co;2-y.
[25] A. Khoshroo, A. Emrouznejad, A. Ghaffarizadeh, M. Kasraei, M. Omid, Sensitivity analysis of energy inputs in crop production using artificial neural networks, J. Clean. Prod. 197 (2018) 992–998, https://doi.org/10.1016/j.jclepro.2018.05.249.
[26] J. Mulongo, M. Atemkeng, T. Ansah-Narh, R. Rockefeller, G.M. Nguegnang, M. A. Garuti, Anomaly detection in power generation plants using machine learning and neural networks, Appl. Artif. Intell. 34 (2020) 64–79, https://doi.org/10.1080/08839514.2019.1691839.
[27] S. Kamnis, K. Malamousi, A. Marrs, B. Allcock, K. Delibasis, Aeroacoustics and artificial neural network modeling of airborne acoustic emissions during high kinetic energy thermal spraying, J. Therm. Spray Technol. 28 (2019) 946–962, https://doi.org/10.1007/s11666-019-00874-0.
[28] M. Barletta, A. Gisario, L. Palagi, L. Silvestri, Modelling the electrostatic fluidised bed (EFB) coating process using support vector machines (SVMs), Powder Technol. 258 (2014) 85–93, https://doi.org/10.1016/j.powtec.2014.03.017.
[29] I.A. Shozib, A. Ahmad, M.S.A. Rahaman, A.M. Abdul-Rani, M.A. Alam, M. Beheshti, I. Taufiqurrahman, Modelling and optimization of microhardness of electroless Ni-P-TiO_2 composite coating based on machine learning approaches and RSM, J. Mater. Res. Technol. 12 (2021) 1010–1025, https://doi.org/10.1016/j.jmrt.2021.03.063.
[30] G. Zhang, S. Guessasma, H. Liao, C. Coddet, J.M. Bordes, Investigation of friction and wear behaviour of SiC-filled PEEK coating using artificial neural network, Surf. Coat. Technol. 200 (2006) 2610–2617, https://doi.org/10.1016/j.surfcoat.2004.12.026.
[31] M. Jiang, C. Ma, F. Xia, Y. Zhang, Application of artificial neural networks to predict the hardness of Ni–TiN nanocoatings fabricated by pulse electrodeposition, Surf. Coat. Technol. 286 (2016) 191–196, https://doi.org/10.1016/j.surfcoat.2015.12.032.
[32] G. Khalaj, Artificial neural network to predict the effects of coating parameters on layer thickness of chromium carbonitride coating on pre-nitrided steels, Neural Comput. Applic. 23 (2013) 779–786, https://doi.org/10.1007/s00521-012-0994-2.
[33] U.M.R. Paturi, N.S.K. Reddy, Experimental investigation to study the effect of electrostatic micro-solid lubricant–coated carbide tools on machinability parameters in turning, Proc. IMechE B J. Eng. Manuf. 229 (5) (2015) 693–702, https://doi.org/10.1177/0954405414530903.
[34] B.M. Greenwell, pdp: an R Package for Constructing Partial Dependence Plots, R J 9, 2017, pp. 421–436, https://doi.org/10.32614/rj-2017-016.